
SUBGROUPTE: ADVANCING TREATMENT EFFECT ESTIMATION WITH SUBGROUP IDENTIFICATION

Seungyeon Lee, Ruoqi Liu
The Ohio State University
{lee.10029, liu.7324}@osu.edu

Wenyu Song
Harvard Medical School
wsong@bwh.harvard.edu

Lang Li
The Ohio State University
Lang.Li@osumc.edu

Ping Zhang*
The Ohio State University
zhang.10631@osu.edu

ABSTRACT

Precise estimation of treatment effects is crucial for evaluating intervention effectiveness. While deep learning models have exhibited promising performance in learning counterfactual representations for treatment effect estimation (TEE), a major limitation in most of these models is that they treat the entire population as a homogeneous group, overlooking the diversity of treatment effects across potential subgroups that have varying treatment effects. This limitation restricts the ability to precisely estimate treatment effects and provide subgroup-specific treatment recommendations. In this paper, we propose a novel treatment effect estimation model, named SubgroupTE, which incorporates subgroup identification in TEE. SubgroupTE identifies heterogeneous subgroups with different treatment responses and more precisely estimates treatment effects by considering subgroup-specific causal effects. In addition, SubgroupTE iteratively optimizes subgrouping and treatment effect estimation networks to enhance both estimation and subgroup identification. Comprehensive experiments on the synthetic and semi-synthetic datasets exhibit the outstanding performance of SubgroupTE compared with the state-of-the-art models on treatment effect estimation. Additionally, a real-world study demonstrates the capabilities of SubgroupTE in enhancing personalized treatment recommendations for patients with opioid use disorder (OUD) by advancing treatment effect estimation with subgroup identification.

Keywords deep learning, treatment effect estimation, subgroup analysis, opioid use disorder

1 Introduction

The primary measure for assessing the effectiveness of interventions is based on the treatment effect (TE), which quantifies the difference in outcomes between the treatment and control groups. The precise estimation of treatment effects is, therefore, of great importance in accurately evaluating the intervention. In recent years, many deep learning models have been proposed and demonstrated remarkable contributions in treatment effect estimation (TEE) [1–6]. These models leverage the power of neural networks to capture intricate relationships among covariates, treatments, and outcomes. Nevertheless, most of these models overlook the existence of heterogeneous subgroups with distinct treatment effects and characteristics, leading to limitations in providing more accurate subgroup-specific estimations and treatment recommendations.

Recognizing the significance of heterogeneity in treatment effects across subgroups is critical, especially considering the diverse nature of populations in real-world situations. Consequently, it is essential to understand and analyze the variability of treatment effects to advance precision treatment. Subgroup analysis aims to identify heterogeneous subgroups with various treatment responses to account for this variability. Nevertheless, existing subgroup identification methods [7–13] have challenges to be addressed. Firstly, most of these methods utilize conventional machine learning

*Corresponding author

models that may encounter challenges when attempting to learn from high-dimensional data with intricate and non-linear relationships among covariates, treatments, and outcomes. Secondly, they highly depend on a one-time pre-estimation of treatment effects to find subgroups whose individuals have similar responses, which can lead to the sub-optimal problem if the pre-estimated effects are inaccurate.

To address the issues, we propose a treatment effect estimation model, called SubgroupTE, that incorporates subgroup identification to find heterogeneous subgroups and learns subgroup-specific causal effects. SubgroupTE advances the estimation of treatment effects by the identified subgroups rather than estimating effects for the entire population. Furthermore, we design an expectation-maximization (EM)-based training process that iteratively optimizes estimation and subgrouping networks to improve estimation and subgroup identification simultaneously. The EM-based training process effectively overcomes the limitations of the pre-estimation step in subgroup analysis, enhancing the overall performance of the model. The SubgroupTE comprises three primary networks: A feature representation network that extracts useful representations from the input data, a subgrouping model that identifies heterogeneous subgroups, and a subgroup-informed prediction network that estimates the treatment effects by considering subgroup-specific causal effects. Specifically, the feature representation network consists of an embedding layer and a Transformer encoder to learn non-linear representations. The subgrouping model pre-estimates the treatment effects and finds subgroups based on the estimated effects. The subgroup-informed prediction network estimates the treatment effects using latent features from the feature representation network and subgroup probabilities from the subgrouping model to consider subgroup-specific causal effects.

Our contributions can be outlined as follows:

- We propose a novel treatment effect estimation model, SubgroupTE, that incorporates subgrouping to identify heterogeneous subgroups and more precisely estimates treatment effects by learning subgroup-specific causal effects.
- We introduce an EM-based training process to iteratively optimize prediction and subgrouping, enhancing both estimation and subgroup identification.
- We demonstrate that considering the heterogeneity of responses within the population leads to more precise predictions compared to estimating treatment effects for the entire population.
- We demonstrate the potential of our method in enhancing treatment recommendations in real-world scenarios.
- We show that SubgroupTE helps to identify the variables contributing to the improvement of treatment effects.

Note that SubgroupTE was introduced in our previous conference paper. The main differences between this paper and the previous conference paper are summarized as follows:

- We perform a robust quantitative analysis, leveraging a semi-synthetic dataset, with state-of-the-art treatment effect and subgrouping models to demonstrate the superiority of SubgroupTE in both treatment effect estimation and subgrouping tasks.
- We conduct an ablation study to evaluate our EM-based training process, demonstrating the strength of iterative optimization for subgrouping and treatment estimation.
- We conduct a sensitivity analysis to assess the impact of the number of subgroups on the prediction performance, demonstrating the significance of identifying subgroups with similar treatment responses and integrating them into the estimation process.
- Code and data are available in a code repository².

2 Related works

This section briefly reviews existing work relevant to our study, including treatment effect estimation and subgroup analysis for treatment effects.

2.1 Treatment effect estimation.

There have been numerous efforts to leverage the power of neural networks in learning counterfactual representations for treatment effect estimation. To successfully apply neural networks for causal inference, it is crucial to design the network structure thoughtfully. Specifically, neural network models are designed to differentiate the treatment variable from other covariates to preserve the treatment-related information in the latent representation. To prevent the loss

²<https://github.com/yeon-lab/SubgroupTE>

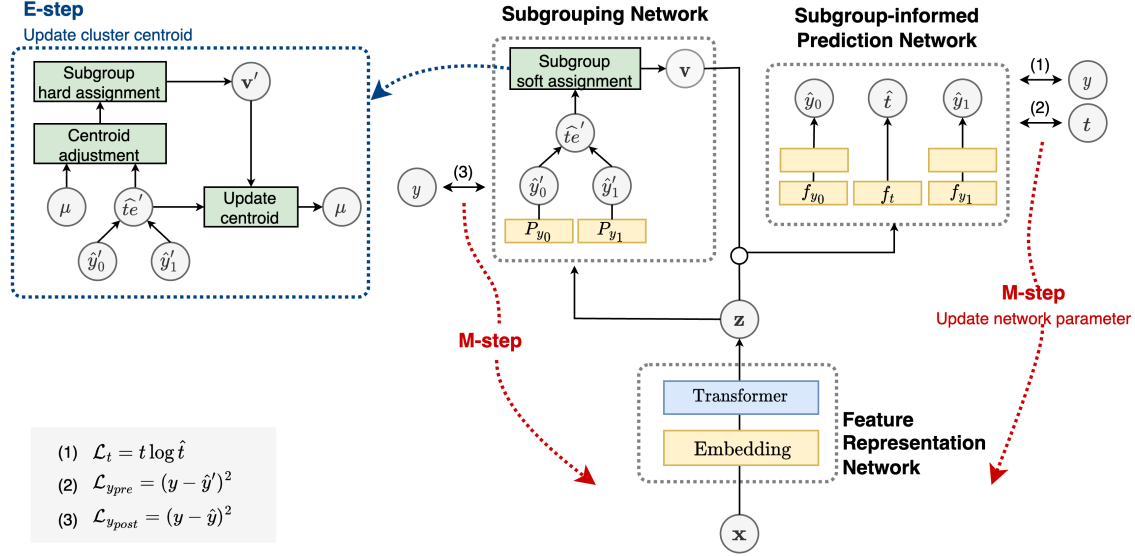


Figure 1: An overview of SubgroupTE.

of treatment information, some previous works [1–4] employ a strategy where covariates from different treatment groups are assigned to separate branches. For example, DragonNet [4] utilizes a shared feature network along with three distinct auxiliary networks, which predict the propensity score, and treated and control outcomes, respectively. By segregating the covariates based on the treatment and utilizing dedicated auxiliary networks, it effectively captures and accounts for the impacts of different treatments. In another effort to avoid loss of treatment information, VCNet [5] maps a real-value treatment to the n -dimensional vector with a mapping function to preserve the treatment information. TransTEE [6] leverages Transformer architecture to capture the interaction between the input treatment and covariates.

Deep learning models have exhibited successful performance in TEE. However, a major limitation in most of these models is that they treat the entire population as a single group, overlooking the diversity of treatment effects across potential subgroups that have varying treatment effects. This can hinder the capacity to precisely estimate treatment effects and provide personalized treatment recommendations for specific subgroups within the population. On the contrary, our novel approach tackles the challenges by incorporating subgroup identification and treatment effect estimation, thereby advancing estimation by considering subgroup-specific causal effects.

2.2 Subgroup analysis

Subgroup analysis for causal inference aims to find subgroups whose individuals have similar treatment responses and/or characteristics. These subgroup analyses are categorized into three distinct groups [14].

Subgrouping with pre-defined hypotheses The approach focuses on analyzing the treatment effect within specific subgroups that are identified based on a priori hypotheses. These hypotheses are formed by considering factors or characteristics that are believed to influence the treatment response.

Directly subgrouping without hypotheses and estimation The approach directly finds subgroups based on statistics, latent patterns, and/or distributions in the data without a priori hypotheses and estimating treatment effect.

Subgrouping with estimated potential outcomes The approach first pre-estimates the potential outcomes and then finds subgroups by maximizing treatment effect heterogeneity/homogeneity across/within subgroups. For example, [7–12] recursively split covariate space into subgroups and find optimal subgroups by maximizing treatment effect heterogeneity. HEMM [13] utilizes Gaussian mixture distributions of subgroups to generate the input, resulting in subject-specific subgroup probabilities. HEMM employs a pre-trained estimation model to learn the parameters of the distributions. The effectiveness of this approach is strongly dependent on the accuracy of the one-time pre-estimation, which may pose challenges in some situations.

Our proposed model belongs to the third category of subgrouping approaches, but it tackles the challenges associated with the one-time pre-estimation. To overcome the challenges, we employ an EM-based training process that iteratively

Table 1: Notation definition

Notation	Description
$D \equiv \{(\mathbf{x}_i, y_i, t_i)\}_{i=1}^{ D }$	input dataset
\mathbf{x}_i	covariate of the i -th patient
y_i	factual outcome
t_i	treatment assignment
\hat{y}_i	prediction of factual outcome
\hat{t}_i	prediction of treatment assignment
$\hat{t}e_i'$	prediction of pre-subgrouping treatment effect
\hat{y}'_0, \hat{y}'_1	prediction of pre-subgrouping control and treated outcomes
\hat{y}_0, \hat{y}_1	prediction of post-subgrouping control and treated outcomes
\mathbf{z}_i	latent representations from Q_ϕ
\mathbf{v}_i	subgroup probability vector
K	the number of subgroups
μ_k	k -th cluster centroid
Q_ϕ	feature representation network
P_{y_0}	subgrouping network for control outcome estimation
P_{y_1}	subgrouping network for treated outcome estimation
f	subgroup-informed prediction network
α, β, γ	weights to control losses

optimizes both subgrouping and treatment effect estimation networks until they converge. This iterative approach leads to enhanced subgroup identification and more precise estimation for each subgroup.

3 Methodology

In this section, we introduce the basic notations, problem formulation, and the proposed framework. We use upper-case and bold letters (e.g., \mathbf{X}) for matrices, lower-case and bold letters (e.g., \mathbf{x}) for vectors, and lower-case letters (e.g., x) for a scalar. Table 1 summarizes the notations used in our study.

3.1 Problem statement

Treatment effect estimation We consider a setting in which we are given a dataset $D \equiv \{(\mathbf{x}_i, t_i, y_i)\}_{i=1}^N$, where N is the number of observed samples. $\mathbf{x}_i \in \mathbb{R}^p$ and $t_i \in \mathbb{R}$ represent p pre-treatment covariates and treatment variable, respectively. t_i is binary when binary treatment setting. The potential outcome y_i indicates the treatment response for t_i of the i -th sample. The propensity score is defined as the conditional probability of the treatment assignment given the observed covariates, represented as $p(t = 1|\mathbf{x})$. Under the potential outcomes framework [15], the treatment effect is defined as the difference between the treated and control outcomes, represented as $\mathbb{E}[Y(1) - Y(0)|\mathbf{x}]$ at a given value of \mathbf{x} . The goal of the prediction model for causal inference is to accurately estimate the treated and control outcomes. With the training data, which includes factual samples \mathbf{x}_i, y_i , and t_i , the model is trained to estimate the factual outcome y_i , given \mathbf{x}_i and t_i .

Following [16], we depend on the assumption of unconfoundedness, which are as follows: (1) Conditional Independence Assumption: The assignment of treatment is independent of the outcome, given the pre-treatment covariates. (2) Common Support Assumption: There is a nonzero probability of the treatment assignment for all samples. (3) Stable Unit Treatment Value Assumption: The observed outcome of each unit remains unaffected by the assignment of treatments to other units. These assumptions are essential in treatment effect estimation as they provide the necessary conditions for unbiased and consistent estimation of causal effects. The assumptions form the basis for our methodology.

Assumption 1 (Ignorability/Unconfoundedness) implies that there are no hidden confounders, such that $Y(0), Y(1) \perp T|X$.

Assumption 2 (Positivity/Overlap) implies that the treatment assignment is non-deterministic, such that $0 < \pi(t|\mathbf{x}) < 1$.

3.2 Proposed model

The proposed model, SubgroupTE, comprises three primary networks: the feature representation network, the subgrouping network, and the subgroup-informed prediction network. The feature representation network, based on the encoder

Algorithm 1: Training process for SubgroupTE

Input: Dataset \mathcal{D} , The number of subgroups K **Output:** Feature representation network Q_ϕ , Subgrouping networks P_{y_0}, P_{y_1} , Subgroup-informed prediction network f , Estimated treatment effect, Subgroups

```
1 for epoch = 1 to  $E$  do
2   for batch  $b = \{(\mathbf{x}_i, y_i, t_i)\}_{i=1}^{|b|}$  in  $\mathcal{D}$  do
3     E-step;
4      $\mathbf{z} = Q_\theta(\mathbf{x})$ 
5      $\hat{t}e' = P_1(\mathbf{z}) - P_0(\mathbf{z})$ 
6     Adjust cluster centroids  $\mu$  using  $\hat{t}e'$  by Eq. (8)
7     Assign clusters  $\mathbf{v}'$  by Eq. (9)
8     Update  $\mu$  by Eq. (10)
9     M-step;
10    Compute subgroup probability  $\mathbf{v}$  by Eq. (3)
11     $\hat{y}, \hat{t} = f(\mathbf{v}, \mathbf{z})$ 
12    Update networks using  $\hat{y}, \hat{t}$  by Eq. (11)
13  end
14 end
```

network of the Transformer model, extracts useful representations from the input data. The subgrouping network pre-estimates the treatment effects and subgroups the data based on the estimated outcomes, generating a subgroup probability vector representing the likelihood of belonging to subgroups. The subgroup-informed prediction network performs the final estimation of the treatment effects, leveraging the latent representation from the feature representation network and subgroup probabilities as input. The SubgroupTE is optimized by the EM-based training, which iteratively updates the cluster centroids for subgrouping and network parameters.

Fig. 1 provides a comprehensive overview of the SubgroupTE framework, highlighting the flow of information and the interactions between the different components. The training process of the proposed method is provided in Algorithm 1.

3.2.1 Feature representation network

To extract latent representations from the input, we employ an embedding layer and encoder network of the Transformer model to construct a feature representation network Q_ϕ . The encoder network consists of self-attention and feed-forward neural networks. Self-attention enables a model to focus on different parts of the input during the encoding process. It allows the model to selectively attend to relevant information at each position

Given the i -th sample \mathbf{x}_i , it is first fed into the embedding layer, and the resulting output is then input into Transformer_Encoder to extract the latent features of \mathbf{x}_i .

$$\begin{aligned} \mathbf{z}_i &= Q_\phi(\mathbf{x}_i) \\ &= \text{Transformer_Encoder}(\text{Embedding}(\mathbf{x}_i)) \end{aligned} \tag{1}$$

3.2.2 Subgrouping model

The goal of the subgrouping model is to identify subgroups of patients that have enhanced or diminished treatment effects. Considering the diverse treatment responses observed among individuals, the subgrouping model aims to capture and account for this heterogeneity by identifying distinct subgroups. To achieve this, the subgrouping network first estimates the control and treated outcomes, denoted as \hat{y}'_0 and \hat{y}'_1 (pre-subgrouping estimations), respectively. This estimation is performed using two distinct one-layer feedforward networks: P_{y_0} and P_{y_1} . These networks take the covariates \mathbf{z}_i as input and predict potential outcomes for the control and treated samples, respectively. The networks have architectures that map the covariates from $\mathbb{R}^{N \times |\mathcal{Z}|}$ to $\mathbb{R}^{N \times 1}$.

The pre-subgrouping treatment effect is then computed for each data sample. Based on the homogeneity of the estimated treatment effects, the subgrouping model assigns a subgroup probability vector to each data sample. The subgroup

probability vector indicates the likelihood of a data sample belonging to each subgroup. It reflects the similarity in treatment effects within subgroups.

The subgroup probability vector, expressed as $\mathbf{v} \in \mathbb{R}^K$, with K representing the number of subgroups, is calculated by measuring the distance between the subgroup centroids and pre-subgrouping treatment effect. Given the i -th sample, the distance d_i^k is computed as the Euclidean distance between the centroid μ_k of subgroup k and \widehat{te}_i as follows:

$$\begin{aligned}\widehat{te}_i' &= P_1(\mathbf{z}_i) - P_0(\mathbf{z}_i) \\ d_i^k &= \left\| \widehat{te}_i' - \mu_k \right\|_2\end{aligned}\tag{2}$$

where $\|\cdot\|_2$ denotes the Euclidean norm.

The probability v_i^k that the i -th sample belongs to the subgroup k is then calculated using the distance d_i^k :

$$v_{i,k} = \frac{\exp^{-d_i^k}}{\sum_{j=1}^K \exp^{-d_i^j}}\tag{3}$$

The probability $v_{i,k}$ is obtained by exponentiating the negative distance d_i^k and normalizing it across all subgroups. The closer the treatment effect \widehat{te}_i' is to the centroid μ_k , the higher the probability $v_{i,k}$ for that subgroup. The subgroup probability vector \mathbf{v}_i is used along with the latent features from the feature representation network as input to the subgroup-informed prediction network. With these subgroup probabilities, the subgroup-informed prediction network can leverage the subgroup information for the treatment effect estimation process, allowing for learning subgroup-specific causal effects.

3.2.3 Subgroup-informed prediction network

The SubgroupTE framework aims to identify heterogeneous subgroups of patients with different treatment effects and improve the precision of outcome estimation by considering subgroup-specific causal effects. To achieve this, the representation vector \mathbf{z}_i and the subgroup probability vector \mathbf{v}_i are concatenated and used as input for the subgroup-informed prediction network.

To ensure the preservation of treatment information in the high-dimensional latent representation, we adapt a strategy where covariates from different treatment groups are assigned to separate branches. The subgroup-informed prediction network f comprises three separate feedforward networks: f_{y_0} , f_{y_1} , and f_t . These networks are responsible for predicting control and treated outcomes, and treatment assignment, respectively. By employing this approach, we ensure that the treatment variable is effectively distinguished from other covariates, thus preserving and incorporating the treatment information into our model. The outputs of the subgroup-informed prediction network are expressed as follows:

$$\hat{y}_{0,i} = f_{y_0}(\mathbf{v}_i, \mathbf{z}_i)\tag{4}$$

$$\hat{y}_{1,i} = f_{y_1}(\mathbf{v}_i, \mathbf{z}_i)\tag{5}$$

$$\hat{t} = f_t(\mathbf{v}_i, \mathbf{z}_i)\tag{6}$$

where $\hat{y}_{0,i}$ and $\hat{y}_{1,i}$ represent the post-subgrouping estimation of control and treated outcomes for i -th sample, respectively, and \hat{t}_i represents the predicted treatment assignment. By incorporating the subgroup probability vector \mathbf{v}_i along with the representation vector \mathbf{z}_i as inputs to the subgroup-informed prediction network, the SubgroupTE framework allows for subgroup-specific treatment effect estimation. This enables a better understanding of the heterogeneity in treatment effects across different subgroups.

3.2.4 Optimization and initialization

To optimize the proposed SubgroupTE model, we employ an expectation–maximization (EM)-based training process, which iteratively optimizes the network parameters and cluster centroids.

In the **E-step**, the cluster centroids are updated while all network parameters are frozen. The K-means algorithm is utilized to assign patients into K subgroups based on the homogeneity of the estimated treatment effects and update cluster centroids. The loss function is as follows:

$$\min_{M \in \mathbb{R}^{K \times 2}} \sum_i \left\| \widehat{te}'_i - v'_i \times M \right\|_2, v'_i \in \mathbb{R}^K \quad (7)$$

where v'_i is a hard assignment vector that assigns each data sample i to one of the K clusters. The centroid matrix M represents the centroids of each cluster, with the k -th row, denoted as μ_k .

Data points are assigned to the nearest clusters based on the distance to their centroids. However, as network parameters are trained, the distribution of the feature space in the network, that is the pre-subgrouping treatment effect estimation, may shift, resulting in discrepancies with the previously updated centroid distribution. This causes the distance between the existing centroids and the data points mapped in the updated feature space to increase. Consequently, some clusters may no longer contain any data points, leading to a reduction in the number of clusters.

To address this issue, we first shift the distribution of the existing centroids to the new feature space before assigning data points to clusters. We accomplish this by computing the Kernel Density Estimation (KDE) of the distribution between the existing centroids and the data points mapped in the new feature space and then updating the centroids using KDE. Specifically, the proposed method includes the following steps. First, we obtain the hidden features in the updated network given the data points. Next, for each centroid, we calculate the KDE between the distributions of the centroid and hidden features. The KDE represents the shift in distribution caused by the changes in the network parameters. Based on the KDE, we update each centroid's position by adjusting it according to the difference in distribution. This adjustment allows the centroids to adapt to the new feature space and ensures that they are representative of the underlying feature distribution. Finally, the data points are assigned to the updated centroids.

The centroids are adjusted as follows:

$$\begin{aligned} \text{Kernel}(\widehat{te}'_i, \mu_k) &= \frac{e^{-\frac{1}{2}((\widehat{te}'_i - \mu_k)/h)^2}}{\sum_i e^{-\frac{1}{2}((\widehat{te}'_i - \mu_k)/h)^2}} \\ \text{Diff}(\widehat{te}'_i, \mu_k) &= \sum_i \text{Kernel}(\widehat{te}'_i, \mu_k) \cdot (\widehat{te}'_i - \mu_k) \\ \mu_k^* &= \mu_k + \text{Diff}(\widehat{te}'_i, \mu_k) \end{aligned} \quad (8)$$

The kernel represents a weight indicating how close each data point is to the cluster center, where a data point closer to the cluster center has a larger value, while a data point farther away has a smaller value. The difference between the data points and each cluster center is then multiplied by its weight, and the sum of these weighted data points over all data points yields the density value. Therefore, $\text{Diff}(\cdot)$ indicates the density distribution of the data points with respect to cluster centers. $\mu_k + \text{Diff}(\cdot)$ adjusts the current position of the cluster center to move towards high-density regions in the feature space.

By aligning the centroids' distribution with the new feature space through KDE-based adjustments before assigning data points to clusters, the proposed method mitigates the issue of decreasing cluster numbers caused by changes in the feature space distribution. The centroid update procedure accounts for the shift in distribution and allows the clusters to adapt to the evolving data representation.

The centroid matrix is then updated using the following equations given a mini-batch. The hard assignment vector v'_i is computed as:

$$v'_{i,j} = \begin{cases} 1, & j = \underset{k \in \{1, \dots, K\}}{\text{argmin}} \left\| \widehat{te}'_i - \mu_k^* \right\|_2, \\ 0, & \text{otherwise.} \end{cases} \quad (9)$$

The centroid is updated as follows:

$$\mu_k = \begin{cases} \frac{1}{|B_k|} \sum_{i \in B_k} \widehat{te}'_i, & |B_k| > 0 \\ \mu_k^*, & \text{otherwise.} \end{cases} \quad (10)$$

where B_k represents all the samples assigned to k -th cluster such that $B_k = \{i \mid \forall i, v_{i,k} = 1\}$.

In the **M-step**, the network parameters are updated. During this step, the cluster centroids are fixed, and a subgroup probability vector \mathbf{v} is assigned to each sample using Eq. (3). The network parameters are subsequently updated using

the predictions from the Subgrouping and Subgroup-informed prediction networks. The loss function is defined as follows:

$$\begin{aligned} \mathcal{L} &= \alpha \cdot \mathcal{L}_t + \beta \cdot \mathcal{L}_{y_{pre}} + \gamma \cdot \mathcal{L}_{y_{post}} \\ &= \alpha \cdot \sum_{i=1}^{|D|} t_i \log \hat{t}_i + \beta \cdot \sum_{i=1}^{|D|} (y_i - \hat{y}'_i)^2 + \gamma \cdot \sum_{i=1}^{|D|} (y_i - \hat{y}_i)^2 \end{aligned} \quad (11)$$

where \hat{y}'_i and \hat{y}_i indicate the pre- and post-subgrouping estimation of i -th sample’s factual outcomes from the subgrouping and subgroup-informed prediction networks, respectively. α , β , and γ are hyper-parameters that control the importance of the treatment assignment, and the pre- and post-subgrouping estimation losses, respectively.

Initialization We leverage k-means++ algorithm [17] to initialize the cluster centroid. It first assigns the first centroid to randomly selected data points from a mini-batch of the input data set. The subsequent centroid is then selected from the remaining data points, with their probabilities determined by the squared distance to the nearest existing centroids. This approach aims to push the centroids as far apart as possible while effectively covering a larger portion of the data space.

4 Experiments

In this section, we assess the performance of the proposed SubgroupTE on two synthetic datasets and compare the results with existing models. Additionally, we demonstrate the practical effectiveness of SubgroupTE in subgroup identification using a real-world dataset.

4.1 Datasets

We conduct our experiments on three datasets including synthetic, semi-synthetic, and real-world datasets. The synthetic and semi-synthetic datasets³, which include true treated and control outcomes, are used to evaluate the treatment effect estimation. In real-world settings, both outcomes are not available. The statistics for the synthetic datasets are described in Table 2.

4.1.1 Synthetic dataset

We simulate a synthetic dataset, following existing works [11, 12]. The dataset is inspired by the initial clinical trial results of remdesivir to COVID-19 [18]. It consists of 10 covariates, which are randomly generated from Normal distribution with different parameter values. The outcomes are simulated using the ‘Response Surface B’ [19]. In total, we generate 1,000 samples, with an even split of 500 case and 500 control samples.

4.1.2 Semi-synthetic dataset

For the semi-synthetic dataset, we utilize the Infant Health and Development Program (IHDP) dataset, which was originally collected from a randomized experiment aimed at evaluating the impact of early intervention on reducing developmental and health problems among low birth weight, premature infants. The dataset consists of 608 control patients and 139 treated patients, totaling 747 individuals, with 25 covariates. The outcomes are simulated based on the real covariates using the ‘Response Surface B’ [19].

4.2 Experimental setup

4.2.1 Baseline models

To assess the prediction performance of SubgroupTE, we conduct comparison experiments with two machine learning-based models, support vector machine (SVR) and random forest (RF), as well as state-of-the-art neural network-based models. The following provides a brief description of these models:

- **DragonNet [4]** consists of a shared feature network and three auxiliary networks that predict propensity score, and treated and control outcomes, respectively.
- **TARNet [3]** consists of a shared feature network and two auxiliary networks that predict treated and control outcomes, respectively.

³The downloadable versions of both synthetic datasets and their simulation can be accessed on our GitHub¹.

Table 2: Statistics on the synthetic and semi-synthetic datasets

Dataset		Synthetic	Semi-synthetic
Number of samples	Total	1000	747
	Case	500	139
	Control	500	608
Avg. of potential outcome	Total	3.93	3.18
	Case	2.34	6.47
	Control	5.48	2.42
Number of features		10	25

- **VCNet** [5] uses separate prediction heads for treatment mapping to preserve and utilize treatment information.
- **TransTEE** [6] leverages the transformer to model the interaction between the input covariate and treatment.

We also conduct comparative experiments with two representative existing subgrouping models to further evaluate the effectiveness of SubgroupTE in subgroup identification. **R2P** [11] is a tree-based subgrouping method, which utilizes a pre-trained treatment effect estimation model to estimate potential outcomes for subgroup identification. **HEMM** [13] utilizes Gaussian mixture distributions to learn subgroup probabilities. HEMM also employs a pre-trained estimation model to learn the parameters of the distributions. R2P and HEMM use the CMGP [20] model and a neural network-based model as treatment effect estimation models, respectively.

4.2.2 Implementation details

All neural network-based models are implemented using PyTorch. We use the SGD optimizer, with a learning rate set to 0.001 and a batch size of 64. The hyper-parameters for the baseline models follow the implementations provided by the respective authors. For our proposed model, we set the hidden nodes from the set {50, 100, 200, 300}, the number of subgroups from the range of [1, 10], and coefficients, which are α , β , and γ , from the range of [0, 1]. The sensitivity analysis for the coefficients and the number of subgroups is shown in Fig. 2.

We perform experiments with a train : dev : test data split ratio of 6 : 2 : 2. The optimal hyper-parameters are found based on the best performance on the validation data. The evaluation metrics are then reported on the test set, providing an unbiased assessment of the model’s performance. We provide a description of optimal hyper-parameters, as well as the computing infrastructure, along with the time/space complexity analysis of the model on our GitHub¹.

4.2.3 Evaluation metric

We employ the precision in estimating heterogeneous effects (PEHE) metric to measure the treatment effect at the individual level, as expressed in Eq. (12). Additionally, we employ the absolute error in average treatment effect (ϵ ATE) to assess the overall treatment effect at the population level, as defined in Eq. (13).

$$\text{PEHE} = \frac{1}{N} \sum_{i=1}^N (f_{y_1}(\mathbf{x}_i) - f_{y_0}(\mathbf{x}_i) - \mathbb{E}[y_1 - y_0 | \mathbf{x}_i])^2 \quad (12)$$

$$\epsilon\text{ATE} = |\mathbb{E}[f_{y_1}(\mathbf{x}) - f_{y_0}(\mathbf{x})] - \mathbb{E}[y_1 - y_0]| \quad (13)$$

To evaluate the performance for subgroup identification, we analyze the variance of treatment effects within and across subgroups. The variance across the subgroups, V_{across} , evaluates the variance of the average treatment effect in each subgroup. On the other hand, the variance within subgroups, V_{within} , measures the mean of the variance of the treatment effects in each subgroup. These metrics are defined as Eq. (14) and Eq. (15), respectively. Here, TE_k indicates a set of the treatment effects in subgroup k .

$$V_{across} = \text{Var}(\{Mean(TE_k)\}_{k=1}^K) \quad (14)$$

$$V_{within} = \frac{1}{K} \sum_{k=1}^K \text{Var}(TE_k) \quad (15)$$

Table 3: Comparison of prediction performance on the synthetic and semi-synthetic datasets. The average score and standard deviation under 30 trials are reported.

Dataset	Model	Synthetic		Semi-synthetic	
		PEHE	ϵ ATE	PEHE	ϵ ATE
ML	RF	0.086 \pm 0.000	0.039 \pm 0.000	0.179 \pm 0.000	0.095 \pm 0.020
	SVR	0.103 \pm 0.000	0.029 \pm 0.000	0.198 \pm 0.000	0.112 \pm 0.023
DL	DragonNet	0.081 \pm 0.013	0.016 \pm 0.013	0.105 \pm 0.037	0.040 \pm 0.010
	TARNet	0.068 \pm 0.010	0.023 \pm 0.003	0.092 \pm 0.019	0.039 \pm 0.010
	VCNet	0.034 \pm 0.005	0.018 \pm 0.010	0.080 \pm 0.031	0.065 \pm 0.049
	TransTEE	0.045 \pm 0.046	0.026 \pm 0.055	0.099 \pm 0.071	0.153 \pm 0.046
	SubgroupTE	0.024 \pm 0.002	0.014 \pm 0.009	0.056 \pm 0.018	0.039 \pm 0.037

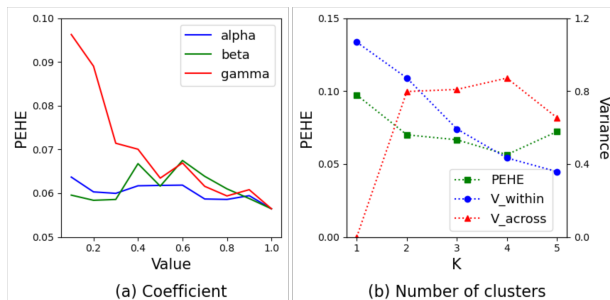


Figure 2: Sensitivity analysis conducted for (a) Coefficient and (b) Number of subgroups on the semi-synthetic dataset. For (a), the performance of each coefficient is evaluated while fixing the remaining two coefficients at 1.

4.3 Results on synthetic data

4.3.1 Treatment effect estimation

Table 3 shows the prediction performance on the synthetic and semi-synthetic datasets. Our proposed SubgroupTE achieves the best performance in both PEHE ϵ ATE compared to other baselines. Notably, it achieves the PEHE of 0.024 and 0.056 on the synthetic and semi-synthetic datasets, respectively, which shows a reduction of 29.4 % and 30.0 % compared to the second-best model. The results demonstrate the effectiveness of SubgroupTE, which integrates subgroup information in the estimation process, thereby enhancing treatment effect estimation.

4.3.2 Subgroup identification

We evaluate whether the model identifies subgroups that maximize heterogeneity between different subgroups while ensuring homogeneity within each subgroup.

Table 4 presents the results of the subgrouping performance on the semi-synthetic dataset. SubgroupTE achieves the best performance compared to all baselines. Both baseline models have lower performance in PEHE, indicating that the pre-trained estimation models are not performing well. As a result, the subgroup performance metrics are shown to be inferior to SubgroupTE. This highlights the limitations of existing subgrouping methods that rely on pre-trained models. In contrast, SubgroupTE demonstrates improved performance in both subgrouping and treatment effect estimation by iteratively training these tasks. Additionally, Fig. 3(b) shows the sensitivity analysis on the number of subgroups. The results demonstrate the significance of identifying subgroups with similar treatment responses and integrating them into the estimation process for treatment effect estimation. When the number of subgroups is 1, treating the entire population as a single subgroup, PEHE is approximately 0.1, similar to other baseline methods. However, as the number of subgroups increases, the PEHE decreases, with the best performance observed when there are 4 subgroups. This further evaluates the effectiveness of our proposed method in effectively identifying diverse subgroups and accurately estimating subgroup-specific treatment effects.

To evaluate whether the model identifies heterogeneous subgroups, we visualize the distributions of the true treatment effects from all subgroups. As shown in Figure 3, SubgroupTE reliably distinguishes heterogeneous subgroups, showing substantial variations in the average treatment effects and clearly separated distributions across different subgroups.

Table 4: Comparison of subgrouping performance on the semi-synthetic dataset.

Model	$V_{within} \downarrow$	$V_{across} \uparrow$	PEHE \downarrow
R2P	0.500 ± 0.15	0.643 ± 0.13	0.154 ± 0.05
HEMM	0.570 ± 0.11	0.591 ± 0.15	0.172 ± 0.00
SubgroupTE	0.393 ± 0.02	0.901 ± 0.01	0.056 ± 0.02

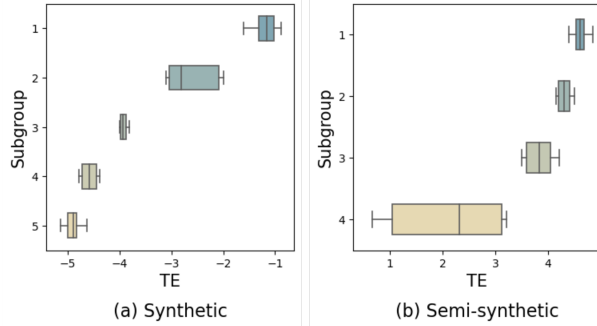


Figure 3: The boxplots of the treatment effect distribution for the identified subgroups on the (a) synthetic and (b) semi-synthetic datasets. The box spans from the first quartile to the third quartile of the data, with a line indicating the median. The whiskers extend from the box to encompass the 5th to 95th percentiles.

The results provide evidence that supports the usefulness of SubgroupTE for subgroup identification, demonstrating its ability to capture and account for the inherent heterogeneity in treatment response within the population.

SubgroupTE iteratively updates cluster centroids and network parameters until they are converged to continuously enhance subgroup identification. Fig. 4 illustrates the trends in PEHE and variance within and across subgroups. As depicted, the variance within subgroups decreases over epochs, while the variance across subgroups increases. These results provide empirical evidence of the continuous improvement in subgroup identification through iterative optimization. Furthermore, it is notable that PEHE decreases over epochs. This demonstrates the mutually reinforcing nature of subgroup identification and treatment effect estimation, indicating that both aspects are effectively learned and improved throughout the training process.

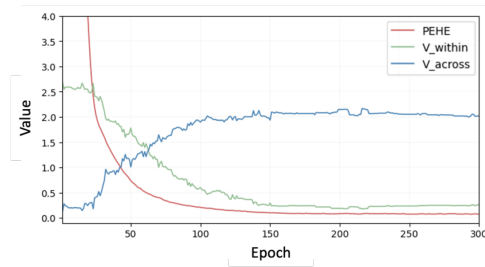


Figure 4: Illustration of the trends in PEHE and variance within and across subgroups during the training phase on the validation set of the synthetic dataset.

4.4 Ablation study

We conduct an ablation study to investigate the effectiveness of the EM-based iterative training process. We compare two variants. **SubgroupTE-O** follows; 1) The model is pre-trained without subgrouping, 2) The cluster centroids are updated and fixed, and 3) The model is re-trained using the subgroup probability derived from the fixed centroids. **SubgroupTE-P** follows; 1) The model is initially pre-trained without subgrouping, and 2) The model parameters and the centroids are iteratively updated. As shown in Table 5, SubgroupTE achieves the highest performance. These findings provide evidence for the effectiveness of our training process, where subgrouping and estimation are learned in a mutually reinforcing manner. Additionally, the results clearly demonstrate that iterative optimization for subgrouping

Table 5: Ablation study for SubgroupTE on the semi-synthetic dataset.

Model	$V_{within} \downarrow$	$V_{across} \uparrow$	PEHE \downarrow
SubgroupTE-O	0.452±0.00	0.854±0.00	0.063±0.00
SubgroupTE-P	0.453±0.01	0.878±0.01	0.060±0.01
SubgroupTE	0.393±0.02	0.901±0.01	0.056±0.02

and treatment estimation enhances estimation accuracy and subgroup identification, overcoming the limitations of the one-time estimation in the existing subgrouping models.

4.5 Real-world study

4.5.1 Problem statement and dataset

Opioid use disorder (OUD) imposes a substantial healthcare and economic burden. Despite various Food and Drug Administration (FDA)-approved drugs for OUD treatment, including Methadone, Buprenorphine, and Naltrexone, they are either restricted in usage or less effective. Naltrexone is accessible through any licensed medical practitioner, whereas Methadone and Buprenorphine require regulatory compliance [21]; Methadone is exclusively accessible through regulated opioid treatment programs (OTPs), and Buprenorphine is prescribable by physicians who have completed specific training or possess addiction board certification and have obtained a federal waiver. Additionally, there exists substantial empirical evidence that supports the effectiveness of medications for OUD (MOUD), particularly Methadone and Buprenorphine [22].

In light of these regulatory and effectiveness considerations, this study aims to compare Naltrexone, a newly approved treatment, with Methadone and Buprenorphine, well-established drugs, to evaluate Naltrexone’s relative efficacy and appropriateness for the treatment of OUD. To conduct this evaluation, the study includes approximately 600,000 patients with OUD from the MarketScan Commercial Claims and Encounters (CCAE) dataset [23], spanning the years 2012 to 2017. The dataset provides comprehensive medical histories for patients, including prescriptions, diagnoses, procedures, and demographic characteristics. We identify OUD patients based on opioid-related emergency department (ED) visits.

4.5.2 Study design

The primary objective of the real-world study is to assess the effect of Naltrexone, compared to Methadone and Buprenorphine, and find subgroups of patients at varying levels of risk for OUD-related adverse events. We collaborated with domain experts to define the adverse outcomes associated with OUD, drawing insights from various studies [24–27]. These events include opioid-related adverse drug events (ORADEs), opioid overdose, and hospitalization. Hospitalization refers to whether a patient is admitted to the hospital after using the drug, and ORADEs and opioid overdose are determined by the presence of corresponding diagnosis codes. Patients who experience any of these adverse events are categorized as "positive," while those who do not are labeled as "negative." To assess Naltrexone’s relative effect compared to Methadone and Buprenorphine, we define case and control cohorts. A case cohort consists of patients prescribed Naltrexone, whereas a control cohort comprises patients prescribed Methadone or Buprenorphine. Detailed selection criteria and statistics are provided in Table 6, and Fig. 5 illustrates the specific criteria.

We construct pre-treatment covariates using diagnosis and medication codes. The diagnosis codes, which are International Classification of Diseases (ICD) codes, are mapped into Clinical Classifications Software (CCS), resulting in 286 unique codes. Additionally, national drug codes (NDCs) of medications are aligned with observational medical outcomes partnership (OMOP) ingredient concept IDs, encompassing 1,353 different drugs. To select the optimal number of subgroups (K), we consider both V_{across} and V_{within} .

4.5.3 Results

In Fig. 3 (b), we present a visualization of the treatment effect distribution for the identified subgroups. Among the identified subgroups, the first subgroup exhibits a positive average treatment effect, suggesting a diminished effect

Table 6: Statistics on the opioid dataset

	$y = 0$	$y = 1$	Total
Case ($t = 1$)	403	353	756
Control ($t = 0$)	1,430	707	2,137
Total	1,833	1,060	2,893

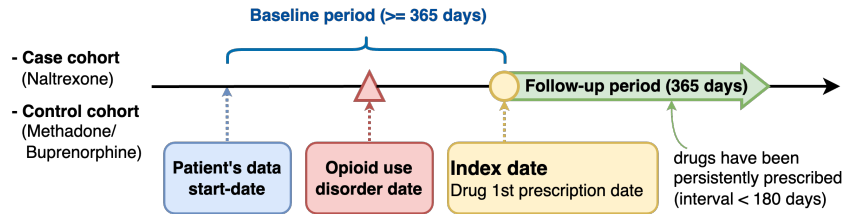


Figure 5: Illustration of the cohort selection criteria. The index date indicates the first prescription date of the drug. The baseline and follow-up periods encompass all dates before and after the index date, respectively.

for Naltrexone within this subgroup. The second subgroup shows an average treatment effect that is close to zero, implying that Naltrexone has minimal impact on the outcomes for these patients. On the other hand, the third subgroup stands out as a notably negative average treatment effect, suggesting that Naltrexone has an enhanced effect compared to Methadone or Buprenorphine. Consequently, Naltrexone might be the preferable treatment option for the third subgroup. Based on these observations, Naltrexone would be most recommended as a treatment option for the third subgroup, where it appears to have the most substantial enhanced effect.

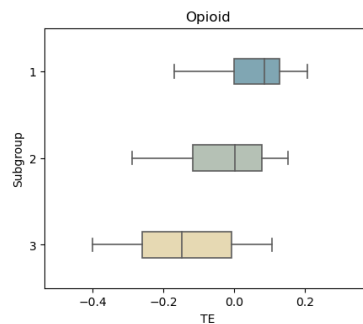


Figure 6: The boxplots of the treatment effect distribution for the identified subgroups on the opioid dataset.

To perform a more comprehensive comparison of the identified subgroups, we analyze the variables related to diagnosis codes and demographics for all subgroups. In Fig. 7, we present a heatmap displaying the relative ratios of the variables for the three subgroups. The ratios are calculated by determining the ratio of each variable within each subgroup and then scaling these ratios across all subgroups. We analyze diagnosis codes recorded only during the baseline period. From the top 15 most frequent codes, we report the 10 codes that exhibit the most differentiation across subgroups. Our analysis reveals intriguing patterns: as the treatment effect improves, the ratios of diagnosis codes typically show a gradual increase or decrease. Furthermore, the third subgroup, which experiences the most significant treatment enhancement, is characterized by a higher proportion of females and younger patients. The findings provide strong evidence that the identified subgroups are indeed clinically distinct. Moreover, they underscore the efficacy of our proposed model in accurately identifying subgroups.

The results indicate the strength of SubgroupTE in identifying subgroups with heterogeneous treatment effects. This demonstrates the advantages of SubgroupTE in developing personalized treatment strategies by not only estimating treatment effects but also recommending a specific treatment for each subgroup. Furthermore, Fig. 7 shows that SubgroupTE effectively understands the characteristics of each subgroup based on patients' medical history and helps to identify the variables contributing to the improvement of treatment effects.

5 Conclusion

This study addresses the critical problems related to treatment effect estimation. We propose a novel framework that incorporates subgrouping and treatment effect estimation to account for the heterogeneity of responses within the population. Through subgroup identification, our model learns subgroup-specific causal effects, thereby advancing treatment effect estimation. We demonstrate the effectiveness of our approach through extensive experiments and analysis. Our model outperforms the state-of-the-art baselines and shows superior performance in both treatment effects

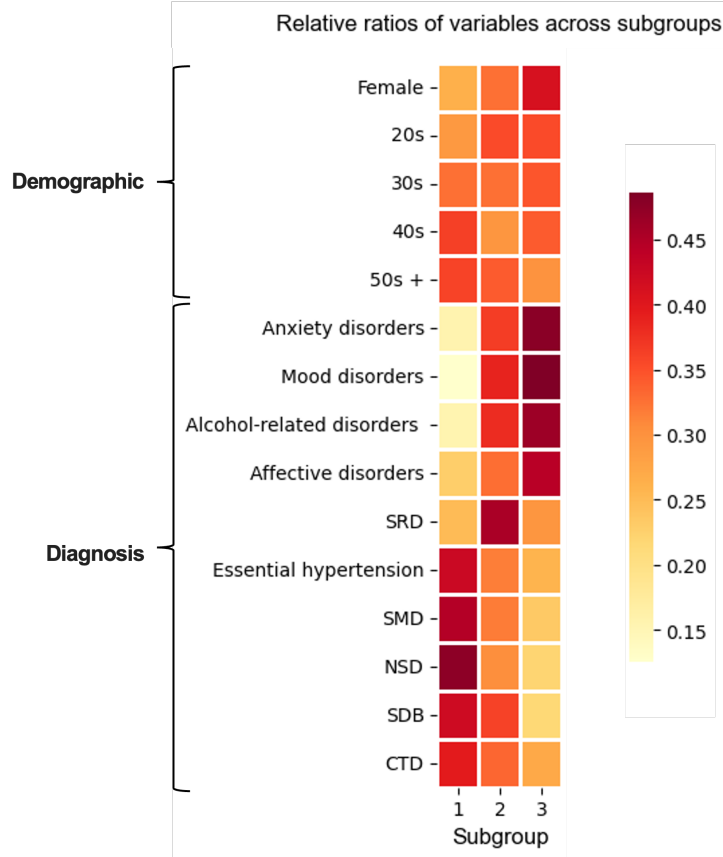


Figure 7: The heatmap of the relative ratios of variables for demographics and diagnosis codes among the three subgroups. These relative ratios are calculated using the formula $\pi_{k,i} / \sum_{k=1}^K \pi_{k,i}$, where $\pi_{k,i}$ represents the ratio of the i -th variable within the k -th subgroup. SMD: Substance-related mental disorders; NSD: Other nervous system disorders; SDB: Spondylosis, intervertebral disc disorders, or other back problems; CTB: Other connective tissue disease.

estimation and subgroup identification. Furthermore, experiments on the real-world dataset demonstrate the potential of our framework in enhancing treatment recommendation and optimization in clinical practice.

References

- [1] Alicia Curth and Mihaela van der Schaar. On inductive biases for heterogeneous treatment effect estimation. *Advances in Neural Information Processing Systems*, 34:15883–15894, 2021.
- [2] Patrick Schwab, Lorenz Linhardt, Stefan Bauer, Joachim M Buhmann, and Walter Karlen. Learning counterfactual representations for estimating individual dose-response curves. In *Proceedings of the AAAI Conference on Artificial Intelligence*, volume 34, pages 5612–5619, 2020.
- [3] Uri Shalit, Fredrik D Johansson, and David Sontag. Estimating individual treatment effect: generalization bounds and algorithms. In *International Conference on Machine Learning*, pages 3076–3085. PMLR, 2017.
- [4] Claudia Shi, David Blei, and Victor Veitch. Adapting neural networks for the estimation of treatment effects. *Advances in neural information processing systems*, 32, 2019.
- [5] Lizhen Nie, Mao Ye, qiang liu, and Dan Nicolae. Vcnet and functional targeted regularization for learning causal effects of continuous treatments. In *International Conference on Learning Representations*, 2021.
- [6] YiFan Zhang, Hanlin Zhang, Zachary Chase Lipton, Li Erran Li, and Eric Xing. Exploring transformer backbones for heterogeneous treatment effect estimation. In *NeurIPS ML Safety Workshop*, 2022.

- [7] Jiabei Yang, Ann W Mwangi, Rami Kantor, Issa J Dahabreh, Monicah Nyambura, Allison Delong, Joseph W Hogan, and Jon A Steingrimsson. Tree-based subgroup discovery in electronic health records: Heterogeneity of treatment effects for dtg-containing therapies. *arXiv preprint arXiv:2208.14329*, 2022.
- [8] Wei-Yin Loh, Haoda Fu, Michael Man, Victoria Champion, and Menggang Yu. Identification of subgroups with differential treatment effects for longitudinal and multiresponse variables. *Statistics in medicine*, 35(26):4837–4855, 2016.
- [9] Jared C Foster, Jeremy MG Taylor, and Stephen J Ruberg. Subgroup identification from randomized clinical trial data. *Statistics in medicine*, 30(24):2867–2880, 2011.
- [10] Kwonsang Lee, Falco J Bargagli-Stoffi, and Francesca Dominici. Causal rule ensemble: Interpretable inference of heterogeneous treatment effects. *arXiv preprint arXiv:2009.09036*, 2020.
- [11] Hyun-Suk Lee, Yao Zhang, William Zame, Cong Shen, Jang-Won Lee, and Mihaela van der Schaar. Robust recursive partitioning for heterogeneous treatment effects with uncertainty quantification. *Advances in Neural Information Processing Systems*, 33:2282–2292, 2020.
- [12] Peniel N Argaw, Elizabeth Healey, and Isaac S Kohane. Identifying heterogeneous treatment effects in multiple outcomes using joint confidence intervals. In *Machine Learning for Health*, pages 141–170. PMLR, 2022.
- [13] Chirag Nagpal, Dennis Wei, Bhanukiran Vinzamuri, Monica Shekhar, Sara E Berger, Subhro Das, and Kush R Varshney. Interpretable subgroup discovery in treatment effect estimation with application to opioid prescribing guidelines. In *Proceedings of the ACM Conference on Health, Inference, and Learning*, pages 19–29, 2020.
- [14] Tong Wang and Cynthia Rudin. Causal rule sets for identifying subgroups with enhanced treatment effects. *INFORMS Journal on Computing*, 34(3):1626–1643, 2022.
- [15] Donald B Rubin. Estimating causal effects of treatments in randomized and nonrandomized studies. *Journal of educational Psychology*, 66(5):688, 1974.
- [16] Michael Lechner. *Identification and estimation of causal effects of multiple treatments under the conditional independence assumption*. Springer, 2001.
- [17] David Arthur and Sergei Vassilvitskii. K-means++ the advantages of careful seeding. In *Proceedings of the eighteenth annual ACM-SIAM symposium on Discrete algorithms*, pages 1027–1035, 2007.
- [18] Yeming Wang, Dingyu Zhang, Guanhua Du, Ronghui Du, Jianping Zhao, Yang Jin, Shouzhi Fu, Ling Gao, Zhenshun Cheng, Qiaofa Lu, et al. Remdesivir in adults with severe covid-19: a randomised, double-blind, placebo-controlled, multicentre trial. *The lancet*, 395(10236):1569–1578, 2020.
- [19] Jennifer L Hill. Bayesian nonparametric modeling for causal inference. *Journal of Computational and Graphical Statistics*, 20(1):217–240, 2011.
- [20] Ahmed M Alaa and Mihaela Van Der Schaar. Bayesian inference of individualized treatment effects using multi-task gaussian processes. *Advances in neural information processing systems*, 30, 2017.
- [21] Anjalee Sharma, Sharon M Kelly, Shannon Gwin Mitchell, Jan Gryczynski, Kevin E O’Grady, and Robert P Schwartz. Update on barriers to pharmacotherapy for opioid use disorders. *Current psychiatry reports*, 19:1–8, 2017.
- [22] Christian Heidebreder, Paul J Fudala, and Mark K Greenwald. History of the discovery, development, and fda-approval of buprenorphine medications for the treatment of opioid use disorder. *Drug and Alcohol Dependence Reports*, page 100133, 2023.
- [23] Marketscan research databases, 2020.
- [24] Richard D Urman, Diane L Seger, Julie M Fiskio, Bridget A Neville, Elizabeth M Harry, Scott G Weiner, Belinda Lovelace, Randi Fain, Jessica Cirillo, and Jeffrey L Schnipper. The burden of opioid-related adverse drug events on hospitalized previously opioid-free surgical patients. *Journal of Patient Safety*, 17(2):e76–e83, 2021.
- [25] Tianyu Sun, Natallia Katenka, Stephen Kogut, Jeffrey Bratberg, Josiah Rich, and Ashley Buchanan. Evaluation of the effectiveness of buprenorphine-naloxone on opioid overdose and death among insured patients with opioid use disorder in the united states. *Pharmacoepidemiology*, 1(3):101–112, 2022.
- [26] Pengyue Zhang, Krystel Tossone, Robert Ashmead, Tina Bickert, Emelie Bailey, Nathan J Doogan, Aimee Mack, Schuyler Schmidt, and Andrea E Bonny. Examining differences in retention on medication for opioid use disorder: An analysis of ohio medicaid data. *Journal of Substance Abuse Treatment*, 136:108686, 2022.
- [27] Victoria D Powell, Colin Macleod, Jeremy Sussman, Lewei A Lin, Amy SB Bohnert, and Pooja Lagisetty. Variation in clinical characteristics and longitudinal outcomes in individuals with opioid use disorder diagnosis codes. *Journal of General Internal Medicine*, 38(3):699–706, 2023.